



## Short communication

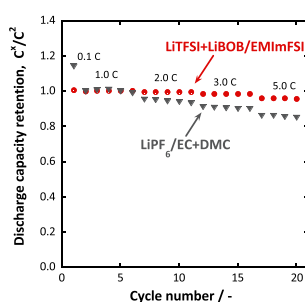
## High-performance graphite negative electrode in a bis(fluorosulfonyl)imide-based ionic liquid

Masaki Yamagata<sup>a,\*</sup>, Yukiko Matsui<sup>a</sup>, Toshinori Sugimoto<sup>a,b</sup>, Manabu Kikuta<sup>c</sup>, Tetsuya Higashizaki<sup>b</sup>, Michiyuki Kono<sup>b</sup>, Masashi Ishikawa<sup>a</sup><sup>a</sup> Department of Chemistry and Materials Engineering, Faculty of Chemistry, Materials and Bioengineering, Kansai University, 3-3-35 Yamate-cho, Suita, Osaka 564-8680, Japan<sup>b</sup> Elexcel Co., Ltd., Laboratory Wing 13F, Keihanna Interaction Plaza, 1-7 Hikaridai, Seika-cho, Soraku-gun, Kyoto 619-0237, Japan<sup>c</sup> Dai-ichi Kogyo Seiyaku Co., Ltd., 5 Ogawa-cho, Kisshoin, Minami-ku, Kyoto 601-8391, Japan

## HIGHLIGHTS

- High-rate capability of a graphite anode can be achieved through the use of an FSI-based ionic liquid electrolyte.
- Highly stable cycling was obtained by the use of the FSI-based ionic liquid electrolyte, even at 60 °C.
- High-performance graphite anode at low-temperature was achieved by using the FSI-based ionic liquid with a LiBOB additive.

## GRAPHICAL ABSTRACT



## ARTICLE INFO

## Article history:

Received 31 October 2012

Accepted 8 November 2012

Available online 19 November 2012

## Keywords:

Lithium-ion battery

Ionic liquids

Bis(fluorosulfonyl)imide

Graphite negative electrode

## ABSTRACT

We evaluated the charge–discharge behavior of a graphite electrode in a 1-ethyl-3-methylimidazolium bis(fluorosulfonyl)imide (EMImFSI) ionic liquid. According to the charge–discharge tests, the graphite negative electrode exhibited a high rate of performance in LiTFSI/EMImFSI (TFSI<sup>−</sup> = bis(trifluoromethylsulfonyl)imide) in the voltage range of 0.005–1.5 V (vs. Li/Li<sup>+</sup>), and the performance was comparable to that in a conventional organic solution-based electrolyte, LiPF<sub>6</sub>/EC+DMC. Moreover, the addition of LiBOB (=lithium bis(oxalato)borate) improved the rate capability and low-temperature operation of the graphite negative electrode, most likely owing to the low-resistivity solid electrolyte interface (SEI) derived from LiBOB. These results suggest that EMImFSI is a suitable electrolyte for lithium-ion batteries utilizing graphite negative electrodes and that optimization of the electrolyte composition with an additive can improve battery performance.

© 2012 Elsevier B.V. All rights reserved.

## 1. Introduction

Recent developments in energy storage systems that deliver large amounts of energy have addressed many limitations impacting mobile equipment, electric vehicles, transportable systems, and small energy grids that employ renewable energy sources. Lithium-

ion batteries are a key technology for realizing a more convenient and sustainable society based on the above-mentioned applications. To ensure the effective use of lithium-ion batteries for such large-scale applications, however, further improvements in safety, energy, and power densities are required, mainly because of the flammable organic solution-based electrolytes used.

Room-temperature ionic liquids, such as 1-ethyl-3-methylimidazolium bis(trifluoromethylsulfonyl)imide (EMImFSI), are attractive candidates for use as the electrolyte in safe lithium-ion batteries because of their diverse properties, such as a wide

\* Corresponding author. Tel./fax: +81 6 6368 1116.

E-mail address: [yamagata@kansai-u.ac.jp](mailto:yamagata@kansai-u.ac.jp) (M. Yamagata).

electrochemical potential window, acceptable ionic conductivity, high thermal stability, and negligible vapor pressure. In particular, such ionic liquids have been considered to improve the safety of lithium-ion batteries due to their lower flammability and lower reactivity compared with conventional organic electrolytes [1–5]. However, lithium-ion batteries composed of ionic liquid electrolytes have serious problems with charge–discharge performance. These problems are due to the significant decomposition of ionic liquids, particularly imidazolium-based liquids, on the negative electrode, leading in most cases to a complete lack of reversibility at the negative electrode. Another problem is the low ionic conductivity of such devices, which results in a lower rate capability [6,7].

Some organic additives, typically ethylene carbonate (EC) and vinylene carbonate, have been introduced into ionic liquid electrolytes to stabilize and protect the interface between the negative carbon electrode and the ionic liquid phase against the undesirable irreversible reactions of ionic liquid components [8–11]. However, despite considerable research into this strategy, there have been few reports of room-temperature ionic liquids that can provide the reversibility of a graphitized negative electrode without the use of additives.

We successfully identified a promising ionic liquid containing bis(fluorosulfonyl)imide (FSI<sup>−</sup>). This liquid with lithium bis(trifluorosulphonyl)imide (LiTFSI) offers reversible charge–discharge properties for negative graphite electrodes without the need for additives, although it contains 1-ethyl-3-methylimidazolium (EMIm<sup>+</sup>), which usually causes irreversible decomposition at graphitic negative electrodes [12,13]. In addition, we investigated the electrochemical behavior of a high-capacitive Si–C composite negative electrode in an FSI-based ionic liquid electrolyte, in which galvanostatic cycling of the negative electrode in the ionic liquid with a charge limitation of 800 mAh g<sup>−1</sup> is stable for 50 cycles [14]. This also reveals that the charge–discharge performance of an attractive cathode, LiNi<sub>1/3</sub>Mn<sub>1/3</sub>Co<sub>1/3</sub>O<sub>2</sub> (NMC), can improve in the FSI-based ionic liquid; the rate capability of the NMC cathode in LiTFSI/EMImFSI clearly exceeds that in conventional LiPF<sub>6</sub>/EC+DMC (DMC = dimethyl carbonate), presumably because of the stable and low-resistivity layer on the NMC [15]. Matsumoto et al. [16–18], Guerfi et al. [19], and Seki et al. [20] also reported the advantages of FSI-based ionic liquids for lithium-metal or lithium-ion batteries.

Regarding the graphite negative electrode, the use of FSI-based ionic liquids for practical purposes necessitates a clarification of the charge–discharge behavior of the graphite negative electrode under various environmental conditions. We report herein the results of a charge–discharge cycle test, an evaluation of the rate characteristics, and high-/low-temperature operation of a graphite negative electrode in combination with an FSI-based ionic liquid. In addition, an additive of lithium salt was considered to improve the low-temperature operation of the negative electrode in this liquid.

## 2. Experimental

EMImFSI was produced by Dai-ichi Kogyo Seiyaku Co. Ltd. The ionic liquid contains less than 10 ppm (w/w) of moisture and less than 2 ppm (w/w) of halides and alkali metal ion impurities. The ionic liquid was dried under vacuum for more than 24 h and preserved in an argon-filled glove box (less than 1.0 ppm of oxygen and moisture). LiTFSI was purchased from Kanto Kagaku Co. Ltd. and was used after drying under vacuum.

We used a graphite powder (Nippon Carbon Co. Ltd.) as an active material, a mixture of a flake graphite and VGCF<sup>®</sup> (Showa Denko K.K.) as a conductive additive, and poly(vinylidene fluoride) (PVdF) as a binder and prepared the composite electrode according to the following procedure. The slurry consisting of uniformly mixed 91 wt.% graphite, 3 wt.% conductive additive, and 6 wt.% PVdF was

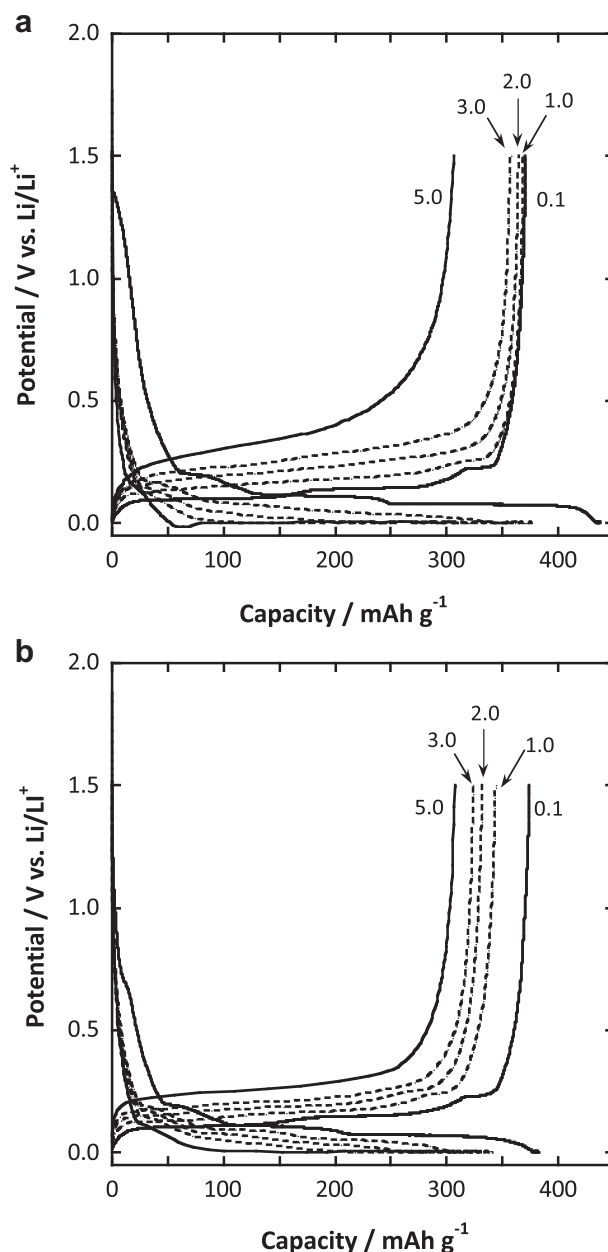


**Fig. 1.** Charge–discharge curves of a graphite negative electrode in (a) LiTFSI/EMImFSI and (b) LiPF<sub>6</sub>/EC+DMC at several charge/discharge C-rates of 0.1/0.1, 1.0/1.0, 2.0/2.0, 3.0/3.0, and 5.0/5.0, with cut-off potentials of 0.005 and 1.5 V vs. Li/Li<sup>+</sup>.

cast on a copper foil and dried overnight under a reduced pressure at 100 °C. The obtained electrode sheet was punched to 1.13 cm<sup>2</sup> in size, and its active layer thickness was 20 μm.

All electrochemical measurements were conducted using a two-electrode half-cell, which consisted of the obtained graphite sheet electrode, 0.45 mol dm<sup>−3</sup> LiTFSI/EMImFSI electrolyte, Li foil (Honjo Metal Co., Ltd) as a counter electrode, and a ceramic-coated separator. The cell was assembled in the glove box after impregnating both the separator and the graphite electrode with the LiTFSI/EMImFSI electrolyte for 30 min under reduced pressure at −0.1 MPa. For comparison, another cell was constructed with a polypropylene separator and a conventional electrolyte of 1.0 mol dm<sup>−3</sup> LiPF<sub>6</sub>/EC+DMC (*v/v* = 1/1) purchased from Kishida Chemical Co. Ltd. To improve the charge–discharge performance, a mixture of 0.45 mol dm<sup>−3</sup> LiTFSI/EMImFSI and 0.01 mol dm<sup>−3</sup> LiBOB/EMImFSI (LiBOB = lithium bis(oxalato)borate) and

a corresponding mixture of 1.0 mol dm<sup>-3</sup> LiPF<sub>6</sub>/EC+DMC with 0.01 mol dm<sup>-3</sup> LiBOB/EC+DMC were prepared.

The charge–discharge performance of the test cells was measured using a computerized battery analyzer (BTS2400W, Nagano Co. Ltd.) in the constant-current/constant-voltage (CC–CV) mode during charging and the CC mode during discharging (the end of the CV mode was defined to be at 1/10 of the set current value) in the voltage range of 0.005–1.5 V (vs. Li/Li<sup>+</sup>). The current density was 0.1 C in the first cycle, following an arbitrary C-rate of charge–discharge repeated after the second cycle. To evaluate the high-/low-temperature operation, the test cells were located in a thermally controlled chamber (SU-241, ESPEC Co.) and the battery analyzer charge–discharge tests were conducted.

### 3. Results and discussion

Fig. 1 shows the charge–discharge curves of the graphite negative electrode in LiTFSI/EMImFSI and LiPF<sub>6</sub>/EC+DMC at charge–discharge rates from 0.1/0.1 to 5.0/5.0 C (1.0 C = 372 mA g<sup>-1</sup>) in the voltage range of 0.005–1.5 V. The discharge capacity of the graphite negative electrode in LiTFSI/EMImFSI at 0.1 C was 371 mAh g<sup>-1</sup>, which is comparable to that in LiPF<sub>6</sub>/EC+DMC. Although the cell with LiTFSI/EMImFSI was found to show curves with larger polarization, it indicated lesser capacity-fading than the cell with LiPF<sub>6</sub>/EC+DMC when the charge–discharge rate increased up to 3.0 C. The dependency of the discharge capacity retention for the graphite negative electrode on the discharge C-rate is summarized in Fig. 2 for both electrolytes. After primary charge–discharge cycling at the 0.1/0.1 C-rate, the rate capabilities of the graphite negative electrode were evaluated by determining the 5-cycle durability for each C-rate operation. The discharge capacity retention was calculated as  $C^x/C^2$ , where  $C^x$  and  $C^2$  are the specific discharge capacities for each cycle ( $x$ ) and for the second cycle (1.0 C-rate), respectively. As shown in Fig. 2, the discharge capacities for both electrolytes gradually decrease as the discharge C-rate increases. A notable feature here is that the rate capability of the graphite negative electrode in a relatively viscous LiTFSI/EMImFSI electrolyte apparently exceeds that in LiPF<sub>6</sub>/EC+DMC up to a 3.0 C-rate. In our second report, which relates the application of an FSI-based ionic liquid to lithium-ion batteries [13],

LiTFSI/EMImFSI forms a lower-resistivity interface between the graphite negative electrode and the electrolyte according to AC impedance analyses. The high retention of the discharge capacity at high C-rates, as presented in Fig. 2, is most likely attributed to the formation of a suitable interface, while the significant loss of capacity retention at a 5.0 C-rate most likely reflects the slow diffusion of charge carriers in the highly viscous ionic liquid.

#### 3.1. High-/low-temperature operation

The effects of temperature on the cyclability of graphite negative electrodes in LiTFSI/EMImFSI and LiPF<sub>6</sub>/EC+DMC were evaluated in the voltage range of 0.005–1.5 V vs. Li/Li<sup>+</sup> at 1.0/1.0 C charging/discharging, as represented in Fig. 3. After pre-cycling at 0.1/0.1 C, the test cells underwent a charge/discharge operation for 9 cycles (1st–9th cycle) at 25 °C, followed by 60 and 0 °C cycling from the 10th to 25th cycle at the same charge–discharge C-rate. During operation at 60 °C (Fig. 3a), the test cell with LiTFSI/EMImFSI achieved a high capacity retention of 0.98 of the initial discharge capacity obtained at 25 °C, whereas that for LiPF<sub>6</sub>/EC+DMC decreased significantly toward 0.78 after 25 cycles, presumably owing to the instability and vaporization of the organic solvents. This suggests that the stable cycling characteristics of the FSI-based ionic liquid are attributed to its nonvolatility and thermal stability, in addition to the formation of a stable solid electrolyte interface layer. Considering the results of the high rate performance of the graphite in the FSI-based liquid, the low-resistivity layer formed on the electrode can offer advantageous low-temperature charge–discharge characteristics. The result for 0 °C cycling shown in Fig. 3b reveals that the cell with LiTFSI/EMImFSI completely lost its discharge capacity, though stable cycling with a capacity retention of approximately 0.8 was obtained for the cell with LiPF<sub>6</sub>/EC+DMC. To clarify the reason for capacity loss in the ionic liquid electrolyte, the lower C-rate charge/discharge behaviors of both cells were evaluated. Comparing the low-temperature performance of the graphite negative electrode under the 0.2/0.2 C charge/discharge operation in both electrolytes (Fig. 3c), the discharge capacity for LiTFSI/EMImFSI reached ~350 mAh g<sup>-1</sup> at the 30th cycle, corresponding to 97% of its discharge capacity measured at 25 °C, and this was relatively larger than that for LiPF<sub>6</sub>/EC+DMC (93%). Such stable and high-capacity retentive cycling of the graphite negative electrode in the FSI-based ionic liquid suggests that the loss of discharge capacity observed during the 1.0/1.0 C charge/discharge measurement described above is due not to electrochemical degradation of the electrolyte or the electrode but a lack of charge carriers inside the electrode derived from the high viscosity of LiTFSI/EMImFSI. The average coulombic efficiency during low-temperature cycling was over 99%, which also proves the absence of any decomposition reactions.

#### 3.2. Additive to stabilize the electrolyte/electrode interface

LiBOB was evaluated as an electrolyte additive with potential to mitigate the disadvantages of FSI-based ionic liquids during low-temperature operation of the graphite negative electrode at 1.0/1.0 C. LiBOB is recognized as a promising electrolyte additive for the formation of an effective solid electrolyte interface (SEI), preventing undesirable reactions and improving thermal stability [21,22]. First, we evaluated the discharge capacity retention of the graphite negative electrode depending on discharge C-rate (0.1–5.0 C) in LiTFSI/EMImFSI and LiPF<sub>6</sub>/EC+DMC with/without 0.5 wt.% LiBOB at 25 °C, and the results are summarized in Fig. 4. The presence of LiBOB in LiPF<sub>6</sub>/EC+DMC caused a slight decrease in the discharge capacitance, especially at 2.0 C or higher, presumably due to an additionally resistive SEI layer derived from LiBOB compared with

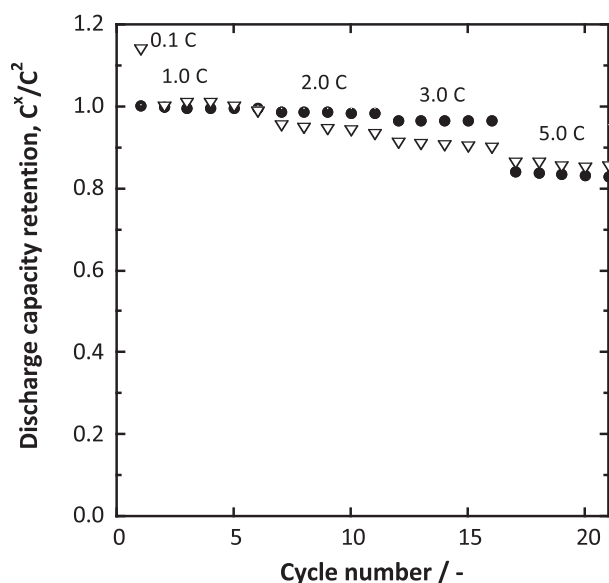
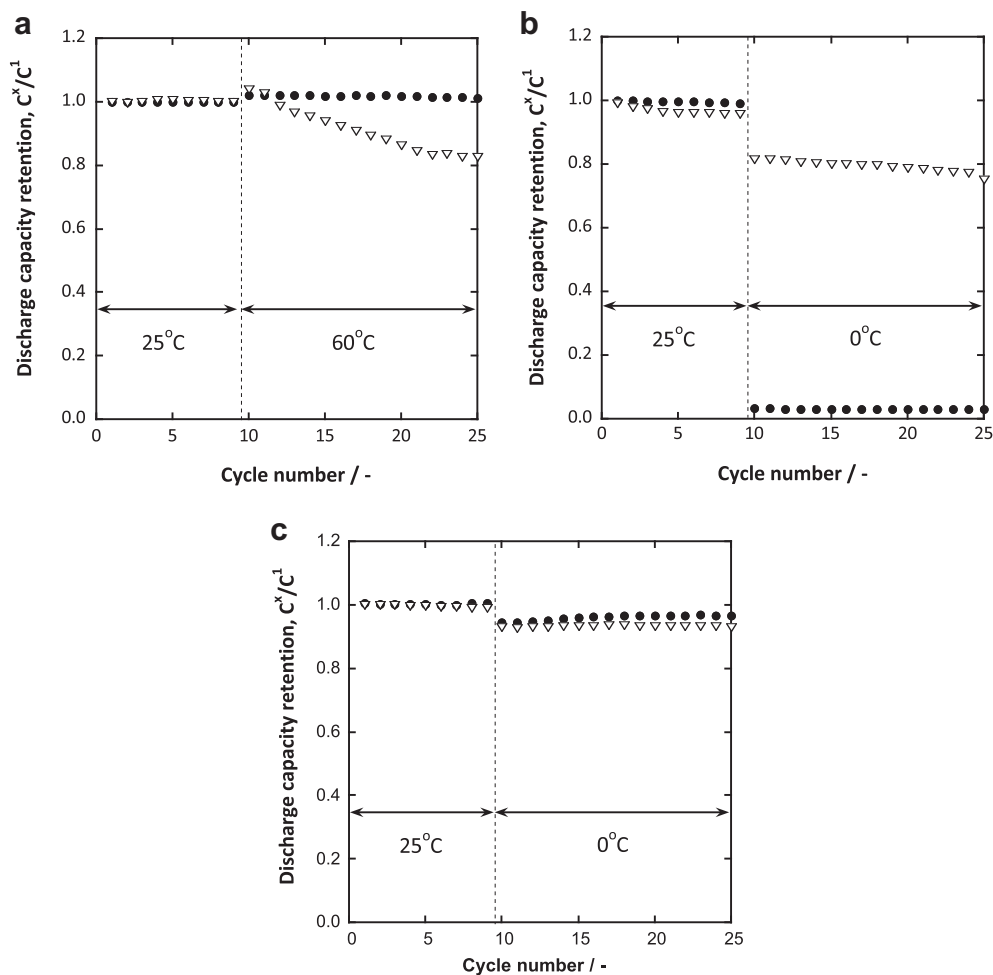


Fig. 2. Rate capability of a graphite negative electrode in LiTFSI/EMImFSI (●) and LiPF<sub>6</sub>/EC+DMC (▽).



**Fig. 3.** Operation temperature dependences of discharge capacity retention of the test cells with LiTFSI/EMImFSI (●) and LiPF<sub>6</sub>/EC+DMC (▽) at (a, b) 1.0/1.0 and (c) 0.2/0.2 charge–discharge C-rates. These test cells were cycled at (a) 60 °C and (b, c) 0 °C after 9 cycles of operation at 25 °C.

that from ethylene carbonate. In contrast, the cell with LiTFSI/EMImFSI dissolving LiBOB demonstrated an enhanced discharge capacity at 5.0 C, in comparison with the LiBOB-free system, and it also exhibited a higher rate capability than that of LiPF<sub>6</sub>/EC+DMC in the whole range of the discharge C-rate. These results suggest that an adequate SEI layer is formed on the surface of the electrode and that it possesses a lower resistivity than those originated by the LiTFSI/EMImFSI and LiPF<sub>6</sub>/EC+DMC electrolytes.

The high rate capability resulting from the addition of LiBOB at 25 °C may improve the low-temperature charge–discharge characteristics of the graphite negative electrode in the FSI-based ionic liquid. Fig. 5 compares the 1.0/1.0 C charge–discharge cycle performance of the test cells with LiTFSI/EMImFSI in the presence/absence of 0.5 wt.% LiBOB at 0 °C. The cell with LiBOB was operable, and its discharge capacity retention at the 25th cycle equaled 67% of the initial capacity measured at 25 °C, which is close to the discharge capacity for a conventional organic electrolyte. We presume that such an absolute improvement in the low-temperature operation, even while using a relatively high-viscosity ionic liquid-based electrolyte, is due to the formation of a stable SEI layer with low resistance derived from the addition of LiBOB; the negligibly thin SEI layer reserves contiguous space and pathways inside the electrode where the charge carriers move smoothly. Meanwhile, in the absence of LiBOB, the interface between graphite and LiTFSI/EMImFSI still contains a layer that slightly inhibits the access of lithium ions to graphite.

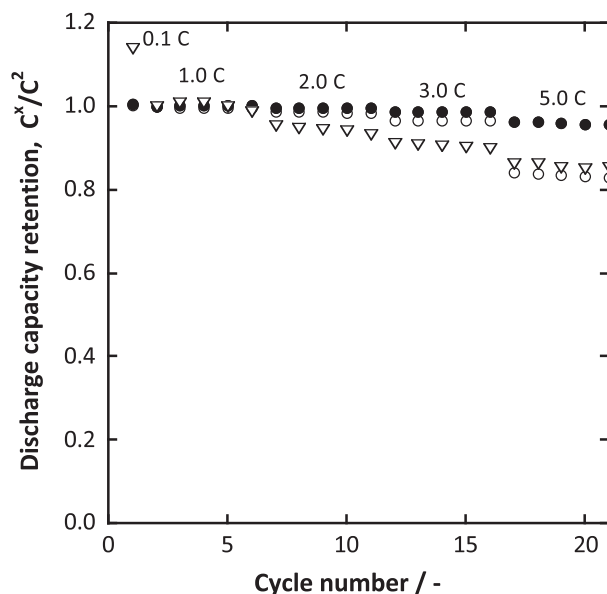


**Fig. 4.** Rate capability of a graphite negative electrode in LiTFSI/EMImFSI with LiBOB added (●), LiTFSI/EMImFSI (○) and LiPF<sub>6</sub>/EC+DMC (▽).

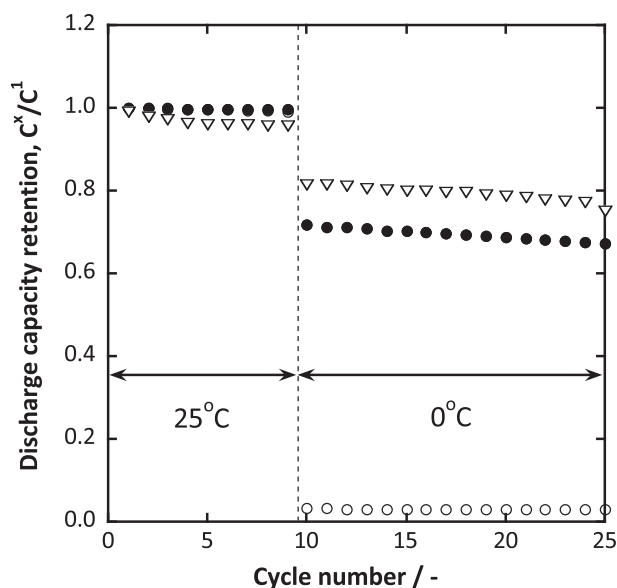


**Fig. 5.** Operation temperature dependences of discharge capacity retention of the test cells for LiTFSI/EMImFSI with LiBOB added (●), LiTFSI/EMImFSI (○), and LiPF<sub>6</sub>/EC+DMC (▽) at 1.0/1.0 C-rate charging–discharging. These test cells were cycled at 0 °C after 9 cycles of operation at 25 °C.

#### 4. Conclusion

The charge–discharge behavior of a graphite negative electrode was investigated in an FSI-based ionic liquid and a conventional organic solution-based electrolyte. The graphite negative electrode demonstrated reversible and stable charge–discharge behavior in the LiTFSI/EMImFSI electrolyte. In particular, the use of the FSI-based ionic liquid made it possible to realize a high rate capability from the graphite negative electrode that was comparable to that of conventional LiPF<sub>6</sub>/EC+DMC, most likely attributable to the low-resistivity interfacial layer. The cell with the nonvolatile LiTFSI/EMImFSI electrolyte exhibited highly stable cycling, even at 60 °C. At low-temperature 1.0/1.0 C charge–discharge operation, however, the cell with LiTFSI/EMImFSI lost its capacity, presumably because the pores inside the electrode were partly filled with layers derived from the ionic liquid, thereby disturbing the access of charge carriers to the graphite active materials. To overcome this disadvantage during low-temperature operation, the introduction of an additive was investigated. The use of LiBOB as an additive for the FSI-based ionic liquid-based electrolyte improved the rate performance of the graphite negative electrode at room temperature and enabled the graphite negative electrode to operate at the low temperature of 0 °C. These results suggest that a type of SEI layer with an extremely low resistance is formed by the addition of

LiBOB and that this thin layer can reserve the contiguous space for the flow of charge carriers into the graphite. There have been no other ionic liquid-based electrolytes that can provide such high-performance of the graphite negative electrode in the FSI-based ionic liquid electrolyte. These advantages suggest that FSI-based ionic liquids are promising electrolytes for safe and high-performance lithium-ion batteries.

#### Acknowledgments

This work was partly supported by a grant from the Development of High-performance Battery Systems for Next-Generation Vehicles Project (Li-EAD Project) from the New Energy and Industrial Technology Development Organization (NEDO), Japan. The authors gratefully acknowledge the foundation support from the Research and Development Organization of Industry–University Cooperation from the Ministry of Education, Culture, Sports, Science and Technology of Japan.

#### References

- [1] R.T. Carlin, J. Fuller, M. Hedenskoog, J. Electrochem. Soc. 141 (1994) L21.
- [2] N. Koura, K. Etoh, Y. Idemoto, F. Matsumoto, Chem. Lett. 2001 (2001) 1320.
- [3] S. Seki, Y. Kobayashi, H. Miyashiro, Y. Ohno, Y. Mita, A. Usami, N. Terada, M. Watanabe, Electrochem. Solid State Lett. 8 (2005) A577.
- [4] S. Seki, Y. Kobayashi, H. Miyashiro, Y. Ohno, A. Usami, Y. Mita, M. Watanabe, N. Terada, Chem. Commun. 2006 (2006) 544.
- [5] T. Sato, T. Maruo, S. Marukane, K. Takagi, J. Power Sources 138 (2004) 253.
- [6] A. Webber, G.E. Blomgren, Ionic liquids for lithium ion and related batteries, in: van W. Schalkwijk, B. Scrosati (Eds.), Advances in Lithium-ion Batteries, Kluwer Academic/Prenum Publishers, 2002, pp. 185–232.
- [7] R.T. Carlin, H.C. De Long, J. Fuller, P.C. Trulove, J. Electrochem. Soc. 141 (1994) L73.
- [8] Y. Katayama, M. Yukumoto, T. Miura, Electrochem. Solid State Lett. 6 (2003) A96.
- [9] M. Holzapfel, C. Jost, P. Novák, Chem. Commun. 10 (2004) 2098.
- [10] M. Holzapfel, C. Jost, A. Prodi-Schwab, F. Krumeich, A. Würsig, H. Buqa, P. Novák, Carbon 43 (2005) 1488.
- [11] H. Zheng, K. Jiang, T. Abe, Z. Ogumi, Carbon 44 (2006) 203.
- [12] M. Ishikawa, T. Sugimoto, M. Kikuta, E. Ishiko, M. Kono, J. Power Sources 162 (2006) 658.
- [13] T. Sugimoto, M. Kikuta, E. Ishiko, M. Kono, M. Ishikawa, J. Power Sources 183 (2008) 436.
- [14] T. Sugimoto, Y. Atsumi, M. Kono, M. Kikuta, E. Ishiko, M. Yamagata, M. Ishikawa, J. Power Sources 195 (2010) 6153.
- [15] Y. Matsui, S. Kawaguchi, T. Sugimoto, M. Kikuta, T. Higashizaki, M. Kono, M. Yamagata, M. Ishikawa, Electrochemistry 80 (2012) 808.
- [16] H. Matsumoto, H. Sakaebe, K. Tatsumi, M. Kikuta, E. Ishiko, M. Kono, J. Power Sources 160 (2006) 1308.
- [17] H. Sakaebe, H. Matsumoto, K. Tatsumi, J. Power Sources 146 (2005) 693.
- [18] H. Sakaebe, H. Matsumoto, K. Tatsumi, Electrochim. Acta 53 (2007) 1048.
- [19] A. Guerfi, S. Duchesne, Y. Kobayashi, A. Viji, K. Zaghib, J. Power Sources 175 (2008) 866.
- [20] S. Seki, Y. Ohno, Y. Kobayashi, H. Miyashiro, A. Usami, Y. Mita, H. Tokuda, M. Watanabe, K. Hayamizu, S. Tsuzuki, M. Hattori, N. Terada, J. Electrochem. Soc. 154 (2007) A173.
- [21] W. Lu, Z. Chen, H. Joachin, J. Prakash, J. Liu, K. Amine, J. Power Sources 163 (2007) 1074.
- [22] C. Täubert, M. Fleischhammer, M. Wohlfahrt-Mehrens, U. Wietelmann, T. Buhrmester, J. Electrochem. Soc. 157 (2010) A721.